Journal of Virology

Chicken Cells Sense Influenza A Virus Infection through MDA5 and CARDIF Signaling Involving LGP2

Matthias Liniger, Artur Summerfield, Gert Zimmer, Kenneth C. McCullough and Nicolas Ruggli

---

Updated information and services can be found at:
http://jvi.asm.org/content/86/2/705

These include:

REFERENCES
This article cites 62 articles, 22 of which can be accessed free at: http://jvi.asm.org/content/86/2/705#ref-list-1

CONTENT ALERTS
Receive: RSS Feeds, eTOCs, free email alerts (when new articles cite this article), more»

Journals.ASM.org

Chicken Cells Sense Influenza A Virus Infection through MDA5 and CARDIF Signaling Involving LGP2

Matthias Liniger, Artur Summerfield, Gert Zimmer, Kenneth C. McCullough, and Nicolas Ruggli

Institute of Virology and Immunoprophylaxis (IVI), Mittelhäusern, Switzerland

Avian influenza viruses (AIV) raise worldwide veterinary and public health concerns due to their potential for zoonotic transmission. While infection with highly pathogenic AIV results in high mortality in chickens, this is not necessarily the case in wild birds and ducks. It is known that innate immune factors can contribute to the outcome of infection. In this context, retinoic acid-inducible gene I (RIG-I) is the main cytosolic pattern recognition receptor known for detecting influenza A virus infection in mammalian cells. Chickens, unlike ducks, lack RIG-I, yet chicken cells do produce type I interferon (IFN) in response to AIV infection. Consequently, we sought to identify the cytosolic recognition elements in chicken cells. Chicken mRNA encoding the putative chicken analogs of CARDIF and LGP2 (chCARDIF and chLGP2, respectively) were identified. HT7-tagged chCARDIF was observed to associate with mitochondria in chicken DF-1 fibroblasts. The exogenous expression of chCARDIF, as well as of the caspase activation and recruitment domains (CARDs) of the chicken melanoma differentiation-associated protein 5 (chMDA5), strongly activated the chicken IFN-β (chIFN-β) promoter. The silencing of chMDA5, chCARDIF, and chIRF3 reduced chIFN-β levels induced by AIV, indicating their involvement in AIV sensing. As with mammalian cells, chLGP2 had opposing effects. While overexpression decreased the activation of the chIFN-β promoter, the silencing of endogenous chLGP2 reduced chIFN-β induced by AIV. We finally demonstrate that the chMDA5 signaling pathway is inhibited by the viral nonstructural protein 1. In conclusion, chicken cells, including DF-1 fibroblasts and HD-11 macrophage-like cells, employ chMDA5 for sensing AIV.

Avian influenza virus (AIV) represents a continuous threat for domestic poultry and humans (7, 34). Both highly pathogenic (HP) and low-pathogenicity (LP) AIV can cause disease in humans (30). Infections with HPAIV cause high morbidity and mortality in gallinaceous poultry but typically do not do so in wild waterfowl (36). Ducks that are infected experimentally with H5N1 do not necessarily develop disease, although virus spreading and shedding can be observed. Knowledge of the innate immune recognition of AIV is crucial to understanding the viral pathogenesis in birds. The recognition of viruses by host cells is mediated by pathogen recognition receptors (PRR) sensing virus-specific pathogen-associated molecular patterns (PAMPs), typically viral nucleic acids. PRR activation results in type I interferon (IFN) induction, cytokine secretion, and the activation of antigen-presenting cells promoting adaptive immune responses (51, 53). PRRs are classified in two main categories: the Toll-like receptors and the retinoic acid-inducible gene I (RIG-I)-like receptors (RLR). RLR are ubiquitously expressed in the cytoplasm (59) and comprise the three helicases RIG-I, melanoma differentiation-associated protein 5 (MDA5), and laboratory of genetics and physiology 2 (LGP2). RIG-I and MDA5 contain two N-terminal caspase activation and recruitment (CARD) domains, a DEX(D/H) box RNA helicase domain, and a C-terminal regulatory or repressor domain (CTD) (9). LGP2 is devoid of CARD domains and therefore lacks signaling capacity (49). It is a positive regulator of the RLR-specific antiviral responses (42, 54). The overexpression of LGP2 can, however, interfere with RLR signaling (40). The RIG-I CTD is involved in viral RNA binding, and the CARDs are required for the interaction with the CARD domain of the mitochondrial adaptor molecule CARDIF, also known as MAVS, IPS-1, or VISA (25, 31, 46, 50, 52, 57). The activation of CARDIF and of the downstream signaling cascade results in the activation of the transcription factors NF-κB and IRF3 and in the secretion of proinflammatory cytokines and type I IFNs (58).

RIG-I was first reported to recognize double-stranded RNA (dsRNA) structures and uncapped 5'-triphosphate (5'-ppp) single-stranded RNA (ssRNA) generated by viral RNA polymerases (18, 38, 60). Later it was found that 5'-ppp recognition by RIG-I requires short blunt 5'-ppp dsRNA, which are contained in panhandle structures of negative-strand RNA viruses (43, 44). MDA5 can be activated by dsRNA, including the synthetic dsRNA analogue p(I:C) (23, 26). Studies conducted with RIG-I-deficient and MDA5-deficient mice demonstrate the essential role of RIG-I for type I IFN induction in response to various negative-strand RNA viruses, while MDA5 senses essentially positive-strand RNA viruses, in particular members of the *Picornaviridae* and *Flaviviridae* families (11, 13, 24, 29). However, MDA5 also can be triggered by certain negative-strand RNA viruses, such as members of the *Paramyxoviridae* family (13) and by AIV (56). Although the RLR pathway generally is conserved among vertebrates, the RIG-I gene could not be identified in chicken (2, 62). Barber and coworkers characterized the duck RIG-I function and suggested that the lack of RIG-I observed in chicken results in a deficiency of the antiviral innate immune response induced by this pathway, possibly explaining the increased susceptibility of chickens compared to that of ducks to AIV (2). Very recently, however, the chicken MDA5 (chMDA5) was identified to mediate type I IFN responses in chicken cells stimulated with synthetic dsRNA (22). This suggests that chickens sense AIV with MDA5. The present study is aimed at characterizing the molecular mechanisms by which chicken DF-1

fibroblast and HD-11 macrophage-like cells sense AIV infections, leading to type I IFN secretion. We show that chMDA5 acts as the chicken PRR responsible for sensing influenza A virus infections in the two chicken cell lines. In addition, we identified chCARDIF, which is essential to mediate chMDA5-dependent type I IFN induction. We also identified chLGP2 and show that it functions as a positive regulator of chMDA5 signaling, similarly to LGP2 in the mammalian RLR pathway. Importantly, the NS1 protein of AIV inhibited the chMDA5 signaling, as is the case for RIG-I signaling in mammalian cells. These data highlight the relevance of the chMDA5 helicase pathway in sensing AIV.

MATERIALS AND METHODS

Cells. DF-1 and HEK293T cells (both from ATCC, Manassas, VA) were propagated in Dulbecco's minimal essential medium (DMEM) plus GlutaMAX-I (Invitrogen) supplemented with 10% heat-inactivated fetal bovine serum (FBS) (Biowest). HD-11 (4) and CEC-32 (45) cells were cultivated in DMEM plus GlutaMAX-I supplemented with 2% chicken serum (Invitrogen) and 8% heat-inactivated FBS. CEC-32 cells carry a luciferase gene under the control of the IFN-responsive chicken Mx promoter and were used to quantify bioactive chicken type I IFN. All avian cells were incubated at 39°C. Madin-Darby canine kidney (MDCK) cells were propagated in MEM with 10% FBS, nonessential amino acids, and 1 mM sodium pyruvate (all from Invitrogen). The stable cell line MDCK-NS1-GFP, expressing influenza A NS1 (kindly provided by Adolfo Garcia-Sastre, Mount Sinai School of Medicine, New York, NY) was propagated in MDCK medium with 0.1 mg/ml hygromycin B (Calbiochem, Basel, Switzerland).

Viruses. A set of eight pHW2000-based plasmids encompassing the gene segments of the LPAIV A/duck/Hokkaido/Vac-1/04 (H5N1) (Vac-1/04) (48) virus was kindly provided by Yoshida Sakoda (Hokkaido University, Sapporo, Japan) with the permission of Robert G. Webster (Department of Infectious Diseases, St. Jude Children's Research Hospital, Memphis, TN). The rescue of viruses from transfected cocultures of HEK293T and MDCK cells was performed as described previously (16) using TransIT-293 (Mirus, Madison, WI). The viruses were amplified in MDCK cells in the presence of 1 μg/ml tosylsulfonyl phenylalanyl chloromethyl ketone (TPCK)-trypsin (Worthington Biochemical, Lakewood, NJ), and the titers were determined as 50% tissue culture infectious doses (TCID$_{50}$/ml) by monitoring the cytopathic effect (CPE) of endpoint dilutions on the same cells. Vac-1/04 virus devoid of the NS1 gene (Vac-ΔNS1) was rescued by transfecting cocultures of HEK293T and MDCK-NS1-GFP cells with the plasmid pHW-2000-NS-V-ΔNS1 (see below) and the seven parent Vac-1/04 plasmids. Vac-ΔNS1 virus stocks were produced and titrated on MDCK-NS1-GFP cells. All experiments with AIV were performed under biosafety level 3 (BSL-3) conditions. Recombinant vesicular stomatitis virus (VSV) replicons devoid of the G surface glycoprotein were packaged into infectious particles using a BHK cell line expressing G glycoprotein. The VSV*M$_Q$ΔG replicon expresses a mutant matrix protein which cannot antagonize the induction of type I IFN (17). The VSV*ΔG(Luc) replicon expressing firefly luciferase was constructed as described elsewhere (3).

Site-directed mutagenesis of NS1. The position of the reported A149V substitution in NS1 (28) corresponds to position 144 in the NS1 of A/chicken/Yamaguchi/7/2004 (H5N1) virus (19). To insert the A144V mutation, the 5′-phosphorylated oligonucleotides Y-NS1mutAV-R and Y-NS1mutAV-F (Table 1 lists all oligonucleotides used for plasmid constructions) were used for PCR with the pHW2000-derived plasmid carrying the Yamaguchi-7/04 NS segment as the template. The religated DNA fragment resulted in plasmid pHW-Y-NS1A144V. The coding regions of Yamaguchi-7/04 NS1 and NS1-A144V were amplified with NS1-Y-L and NS1-VY-R and cloned with BamHI and EcoRI into pcDNA6-V5-His B (Invitrogen). The Vac-1/04 NS1 and NS1-A149V expression plasmids were cloned accordingly. For the NS1-deficient construct, the pHW2000-

derived plasmid carrying the Vac-1/04 NS segment served as the template in a PCR using the 5′-phosphorylated oligonucleotides dNS1-V-R and dNS1-V-L. The product was ligated to obtain plasmid pHW-2000-NS-V-ΔNS1.

SDS-PAGE and Western blotting. Cells were lysed in a hypotonic buffer containing 20 mM morpholinepropanesulfonic acid, 10 mM NaCl, 1.5 mM MgCl$_2$, 1% Triton X-100 (pH 6.5), and protease inhibitor cocktail (Sigma). Proteins were separated by SDS-PAGE under reducing conditions and analyzed by Western blotting (41) using anti-V5 (Invitrogen), anti-HaloTag (Promega), or anti-β-actin (C4) antibodies (Santa Cruz) and IRDye-labeled secondary antibodies (Li-Cor Biosciences). The signals were acquired and quantified using the Odyssey infrared imaging system (Li-Cor Biosciences).

Design of chicken IFN-β and Mx promoter reporter plasmids. The chicken IFN-β promoter (GenBank accession no. Y14969.1) (47) and Mx promoter (GenBank accession no. EF487534.1) were amplified from White Leghorn chicken genomic DNA by PCR using the oligonucleotides ch-P-IFNb-L and ch-P-IFNb-R or ch-P-Mx-L and ch-P-Mx-R, respectively. The fragments were cloned with SmaI and HindII to replace the mouse Mx promoter in pGL3-Mx1P-FF-Luc (a kind gift of Georg Kochs, Department of Virology, University of Freiburg, Germany) (20), resulting in pGL3-P-chIFN-β-luc and pGL3-P-chMx-luc.

Preparation and enzymatic treatments of RNA stimuli. Polyinosinic-poly(C) [p(I:C)] sodium was purchased from Sigma. The production of in vitro-transcribed RNA (IVT-RNA) was performed as described previously (18), with minor modifications. HindIII-linearized pBluescriptII SK+ served as the template using the MEGAscript T7 kit (Ambion). After DNase I treatment, the IVT-RNA was purified using Mini-Quick Spin Oligo Columns (Roche). Corresponding synthetic ssRNA (51 nucleotides) devoid of 5′-ppp structures was obtained from Microsynth (Balgach, Switzerland). For dephosphorylation, 15 μg of RNA was treated with 200 U of calf intestinal alkaline phosphatase (CIP; Promega). RNA digestions (15 μg) were performed using an RNase cocktail (Ambion) in 100 mM NaCl, 50 mM Tris-HCl, 10 mM MgCl$_2$, 1 mM dithiothreitol (pH 7.9) for 2 h at 37°C. All reaction mixtures were heat inactivated at 65°C for 15 min and purified twice using Mini-Quick Spin Oligo columns (Roche).

Transient promoter reporter assays in chicken DF-1 cells. To determine chicken IFN-β and Mx promoter activities, DF-1 cells grown in 96-well plate format at 2×10^4 to 4×10^4 cells/well were cotransfected with 25 to 50 ng/well of pGL3-P-chIFN-β-luc or pGL3-P-chMx-luc and 0.1 ng/well of a plasmid constitutively expressing Renilla luciferase (phRL-SV40; Promega) using Fugene HD (Roche). HEK293T cells were transfected with plasmid p125Luc (61) and phRL-SV40. Cells were lysed using 20 μl of 1× passive lysis buffer (Promega), and samples were assayed for firefly and Renilla luciferase activity using the dual-luciferase reporter assay system (Promega) and a Centro LB 960 luminometer (Berthold Technologies).

Chicken type I IFN bioassay. Bioactive type I chicken interferon (IFN) was measured using CEC-32 reporter cells (kindly provided by Peter Staeheli) adapted to 96-well plate format (33, 45). To avoid interference with the bioassay, p(I:C) and IVT-RNA were removed from DF-1 or HD-11 cells after 3 h. Virus interference was avoided by the heat inactivation of the samples at 65°C for 30 min, which did not influence type I chIFN bioactivity.

Cloning of the putative chCARDIF. A BLASTP search of the RefSeq chicken protein database at NCBI using the murine CARDIF protein sequence (NCBI NP_659137.1) retrieved a protein sequence of 641 amino acids with unknown function, designated hypothetical protein LOC422936 (NP_001012911.1) (6). The corresponding cDNA sequence (GenBank no. NM_001012893.1) was used to design the oligonucleotides ch-CARDIF-L and ch-CARDIF-R for reverse transcription-PCR (RT-PCR) from chicken spleen RNA. The PCR fragment was cloned into pCR4-TOPO and transferred with KpnI and EcoRI to pcDNA6-V5-His B. The nucleotide sequence of the putative chCARDIF was

TABLE 1 Oligonucleotides used for plasmid constructions

Name	Sequence (5′–3′)
Y-NS1mutAV-R[a]	TCCTTCTTCTGTGAAAACTCTAAG
Y-NS1mutAV-F[a]	GCAATCGTGGGAGAAATCTCAC
NS1-Y-L[a]	ATTGGATCCACCATGGATCTCAACACTGTGTCAAG
NS1-VY-R[a]	CATGAATTCTTATCAAACTTCTGACTCAATTGTTC
dNS1-V-R[a]	CTGAAAGCTTGACACAGTGTTGG
dNS1-V-L[a]	GACATACTGATGAGGATGTC
ch-P-IFNb-L[a]	TAGCCCGGGCTCCCACTCTGGTTGCATCAG
ch-P-IFNb-R[a]	TAGAAGCTTAACCTTGGTGGGACTTGTGTTC
ch-P-Mx-L[a]	TAGCCCGGGTCGGTGTCACATCCACACGG
ch-P-Mx-R[a]	TAGAAGCTTCTGCCAGAGTCACACAGCAAG
ch-CARDIF-L[a]	ATAGGTACCACCATGGGTTTCGCCGAGGACAAAG
ch-CARDIF-R[a]	CATGAATTCCTATTTCTGCAATCGTGTGTACAC
N-chCARDIF-F[a]	TATAGCGATCGCCATGGGTTTCGCCGAGGACAAAG
N-chCARDIF-R[a]	CCATGTTTAAACCTATTTCTGCAATCGTGTGTACAC
N-d-chCARD-F[a]	TATAGCGATCGCCATGCAGAACAATGCAGGGCACCTGG
d-chTM-R[a]	CCATGTTTAAACCTACGGCCCATTGCTGTCCCCTG
Halo-ctrl-F[a]	CGCCTGATAGCTAACTGAGTTT
Halo-ctrl-R[a]	AAACTCAGTTAGCTATCAGGCGAT
ch-IRF-3-L[a]	ATAAAGCTTGCCACCATGGCAGCGCTGGACAGCG
ch-IRF-3-R[a]	CATGAATTCAGTCTGTCTGCATGTGGTATTG
ch-MDA5-L[a]	ATAAAGCTTGCCACCATGGTACACGTCAGTTTTGTTTTC
chMDA5-BamHI-R[a]	GATCTCAATAATTCTTTCTCTAAATG
chMDA5-int-L[a]	GTCAGAGAGAGCAGTGTATTGG
ch-MDA5-R[a]	CATGTTTAAACTTAATCTTCATCACTTGAAGGACA
chRLRlgp2-F-HindIII[a]	TATAAAGCTTATGGAGCTCCACGGGTACCAAC
chRLR_R_Stop_BamHI[a]	GCATGGATCCCTACAGGGACTCGTCCTGAGTG
hRIG-I-L[a]	ATAAAGCTTGCCACCATGACCACCGAGCAGCGACGCAG
hRIG-I-R[a]	TTACTCGAGTCATTTGGACATTTCTGCTGGATC
huMDA5-L[a]	ATAGGTACCACCATGTCGAATGGGTATTCCACAG
huMDA5-S-R[a]	TTACTCGAGCTAATCCTCATCACTAAATAAACAGC
1hp-L[b]	ggcggggctagctggagaagatgccttccggagaggtgctgctgagcg
1hp-R[b]	gggtggacgcgtaagaggggaagaaagcttctaaccccgctattcaccaccactaggca
CTRL-sh-F[b]	gagaggtgctgctgagcgaAGGTAGTGTAATCGCCTTGCAtagtgaagccacagatgta
CTRL-sh-R[b]	attcaccaccactaggcaCAGGTAGTGTAATCGCCTTGCAtacatctgtggcttcact
chMDA5-sh3-F[b]	gagaggtgctgctgagcgaGAGCAGAATAGTGCAGAAGAAtagtgaagccacagatgta
chMDA5-sh3-R[b]	attcaccaccactaggcaTGAGCAGAATAGTGCAGAAGAAtacatctgtggcttcact
chCARDIF-sh3-F[b]	gagaggtgctgctgagcgaTCAGCTCCTCCAAGTGCTTCAtagtgaagccacagatgta
chCARDIF-sh3-R[b]	attcaccaccactaggcaCTCAGCTCCTCCAAGTGCTTCAtacatctgtggcttcact
chIRF3-sh3-F[b]	gagaggtgctgctgagcgcGTCCAAGCTCATCCTGGTGAAtagtgaagccacagatgta
chIRF3-sh3-R[b]	attcaccaccactaggcaAGTCCAAGCTCATCCTGGTGAAtacatctgtggcttcact

[a] Oligonucleotides used for PCR-based cloning.
[b] Oligonucleotides used for the construction of pRFPRNAiC-derived plasmids for the expression of short hairpin RNA (the target sequence is marked in capitals). The 5′ base of the sense strands (underlined in the oligonucleotide sequences) were modified to form mismatches to mimic the endogenous miRNA30.

determined from both strands of two independent clones (GenBank no. HQ845772). The sequence was found to be identical to GenBank no. NM_001012893.1.

Construction of plasmids encoding untagged or N-terminally HT7-tagged chCARDIF and deletion mutants thereof. The chCARDIF open reading frame (ORF) was amplified by PCR using the oligonucleotides N-chCARDIF-F and N-chCARDIF-R. A chCARDIF lacking the putative N-terminal CARD domain was designed using the oligonucleotides N-d-chCARD-F and N-chCARDIF-R. A deletion mutant devoid of the putative C-terminal transmembrane domain (TM) was constructed using the oligonucleotides N-chCARDIF-F and d-chTM-R. A further double deletion construct, lacking the CARD and the TM domains, was generated with the oligonucleotides N-d-chCARD-F and d-chTM-R. To generate N-terminally HaloTag 7 (HT7)-tagged proteins, the different chCARDIF fragments were inserted in pFN21K-HT7-CMV (Promega) between the AsiSI and PmeI sites. A control plasmid for the expression of the HT7 tag alone was constructed by ligating a DNA cassette composed of the annealed 5′-phosphorylated oligonucleotides Halo-ctrl-F and Halo-ctrl-R

into the SgfI and PmeI sites of pFN21K-HT7-CMV. To obtain the corresponding untagged constructs, the pFN21K-HT7-CMV-derived constructs were digested with the restriction endonucleases NheI and XhoI, and the overhangs were filled in with the large Klenow fragment of DNA polymerase I (New England BioLabs) before religation and sequence verification.

chCARDIF localization study. The plasmid pHcRed1-Mito (Clontech), encoding far-red fluorescent protein HcRed1 fused to the mitochondrial targeting sequence of the human cytochrome *c* oxidase subunit VII, was used to label mitochondria. DF-1 cells were cotransfected with pHcRed1-Mito and plasmids encoding N-terminally HT7-tagged chCARDIF or deletion mutants thereof. The next day, the cells were treated with the green fluorescent HaloTag R110 direct ligand (Promega) to stain the HT7-tagged proteins, as described by the manufacturer. Image acquisition employed a Leica TCS-SL spectral confocal microscope together with Leica LCS software (Leica Microsystems AG). Images were analyzed and micrographs prepared using the Imaris 7.2 software program (Bitplane AG).

TABLE 2 Sequences of siRNAs used for silencing and of primers and probes used for quantitative real-time RT-PCR

Name	Sequence[a] (5′–3′)	Application
CTRL-siRNA	AGGUAGUGUAAUCGCCUUG	siRNA
chMDA5-siRNA2	AAGAAGGGAUCCAUUUAGA	siRNA
chMDA5-siRNA3	AUAUAAUGAUGCUCUGCAA	siRNA
chCARDIF-siRNA2	UGCUGCAGGAAGCUUUGAA	siRNA
chLGP2-siRNA1	UGGAGAUGAUCUACCGGAA	siRNA
Avi18S-F	TCCCCTCCCGTTACTTGGAT	RT-PCR
Avi18S-R	GCGCTCGTCGGCATGTA	RT-PCR
Avi18S-P	FAM-ACTGTGGTAATTCTAGAGCTA-BHQ1	RT-PCR
chIFN-β-F	CCTCCAACACCTCTTCAACATG	RT-PCR
chIFN-β-R	TGGCGTGCGGTCAAT	RT-PCR
chIFN-β-P	FAM-TTAGCAGCCCACACACTCCAAAACACTG-TAMRA	RT-PCR
chMDA5-F	GGACGACCACGATCTCTGTGT	RT-PCR
chMDA5-R	CACCTGTCTGGTCTGCATGTTATC	RT-PCR
chMDA5-P	FAM-CAGCTGCTGCACGGCACGCT-BHQ1	RT-PCR
chCARDIF-F	CACCCACGAGGTCCATGTG	RT-PCR
chCARDIF-R	TGCTTCATCTGGGACATCATTG	RT-PCR
chCARDIF-P	FAM-CATCACCCCAGTGCCCCGCTC-BHQ1	RT-PCR

[a] FAM, 6-carboxyfluorescein; BHQ1, black hole quencher 1; TAMRA, 6-carboxytetramethylrhodamine.

Cloning of chMDA5, putative chLGP2, and chIRF3. chMDA5 was cloned based on the GenBank no. XM_422031.2 sequence. The N-terminal fragment was amplified with the oligonucleotides ch-MDA5-L and chMDA5-BamHI-R and was cloned with HindIII and BamHI into pcDNA6-V5-His B. The C-terminal part was amplified with chMDA5-int-L and ch-MDA5-R. The plasmid pcDNA6-chMDA5 was obtained by cloning the BamHI- and PmeI-digested C-terminal fragment into the BamHI and EcoRV sites. Sequence analysis of three independent clones revealed a histidine-to-arginine change at position 477 (H477R) compared to the published chMDA5 (8) and NP_001180567.1 sequences. To express the CARD domains of chMDA5, a fragment encoding the N-terminal 642 amino acids was obtained by RT-PCR using the oligonucleotides ch-MDA5-L and chMDA5-BamHI-R and cloned into the HindIII and BamHI sites of pcDNA6-V5-His B. The putative chLPG2 terminal sequences were identified based on similarities to mammalian LGP2 sequences. The putative chicken LGP2 (chLGP2) was cloned by RT-PCR using the oligonucleotides chRLRlgp2-F-HindIII and chRLR-R-Stop-BamHI. The HindIII- and BamHI-digested PCR fragment was ligated into the respective sites of pcDNA6-V5-His B. The nucleotide sequence of chLGP2 was determined from two strands of two independent clones and deposited in GenBank (HQ845773). The chIRF3 gene (14) was amplified from chicken spleen RNA by RT-PCR using the oligonucleotides ch-IRF-3-L and ch-IRF-3-R and was cloned into the HindIII and EcoRI sites of pcDNA6-V5-His B. The full-length human RIG-I (huRIG-I) and MDA5 (huMDA5) were originated from plasmids kindly provided by Ralf Bartenschlager, Department of Molecular Virology, University of Heidelberg, Germany (5). All plasmid inserts were sequenced.

Expression of shRNA and siRNA transfection. For specific gene knockdown in chicken cells, pRFPRNAiC-based silencing (ARK-Genomics, Scotland, United Kingdom) was applied (10). The 22-nucleotide RNA interference (RNAi) target sequences were designed using the Genscript RNAi target finder (https://www.genscript.com/ssl-bin/app/rnai). Hairpins to clone into the microRNA (miRNA) cloning site were generated by PCR using random and gene-specific oligonucleotides together with 1hp-L and 1hp-R (Table 1). The control short hairpin RNA (shRNA) (CTRL-sh) sequence was derived from a random short interfering RNA (siRNA) designed by Microsynth (Balgach, Switzerland). The PCR products were cloned with NheI and MluI into pRFPRNAiC. Double-stranded siRNAs (21-mers with TT overhangs at the 3′ ends) were designed and purchased as annealed duplexes from Microsynth (Table 2). For silencing, DF-1 or HD-11 cells were transfected with siRNAs at a 100 nM final concentration using TransIT-TKO (Mirus) according to the manufacturer's protocol.

Real-time quantitative RT-PCR. RNA was extracted using TRIzol (Invitrogen), DNase I (Ambion), and RNase inhibitor (RNasin Plus; Promega) or with the Nucleospin RNA II kit (Macherey-Nagel) and amplified with the SuperScript III platinum one-step quantitative RT-PCR system (Invitrogen) using oligonucleotide primers and probes (Table 2) purchased from Microsynth. Primers and probes for chIFN-β were published earlier (37). As an internal standard, the primers Avi18S-F and Avi18S-R and the probe Avi18S-P, specific for the chicken 18S rRNA, were used (GenBank no. AF173612.1).

Nucleotide sequence accession number. The nucleotide sequences of the open reading frames of the putative chCARDIF and chLGP2 have been deposited in GenBank under accession numbers HQ845772 and HQ845773.

RESULTS

Chicken DF-1 and HD-11 cells can be stimulated with dsRNA and IVT-RNA to produce type I interferon. To characterize the response of chicken cell lines to stimulation with RNA mimicking the danger signals associated with viral infections, DF-1 fibroblast cells and HD-11 macrophage-like cells were stimulated with dsRNA and 5′-triphosphorylated ssRNA analogues. DF-1 cells responded to transfected p(I:C) [t-p(I:C)] and to transfected 5′-triphosphorylated IVT-RNA (t-IVT-RNA) with a strong IFN-β promoter induction, similarly to the case for the human HEK293T cell line (Fig. 1A and B). Accordingly, bioactive type I chIFN was detected in the supernatant of DF-1 and HD-11 cells, with a 10-fold higher response measured in HD-11 cells (Fig. 1C and D). The transfection of all cell lines with ssRNA of the same sequence as the IVT-RNA but devoid of 5′ triphosphates did not induce any detectably type I IFN response (Fig. 1A to G).

Chicken cells respond to dephosphorylated IVT-RNA, unlike HEK293T cells. As expected from previous reports (18), IVT-RNA from which the 5′-ppp were removed enzymatically lost their ability to activate the IFN-β promoter in human HEK293T cells (Fig. 1E). Surprisingly, the CIP treatment of IVT-RNA did not alter the capacity of t-IVT-RNA to induce the chIFN-β promoter in DF-1 cells and type I chIFN secretion in HD-11 cells (Fig.
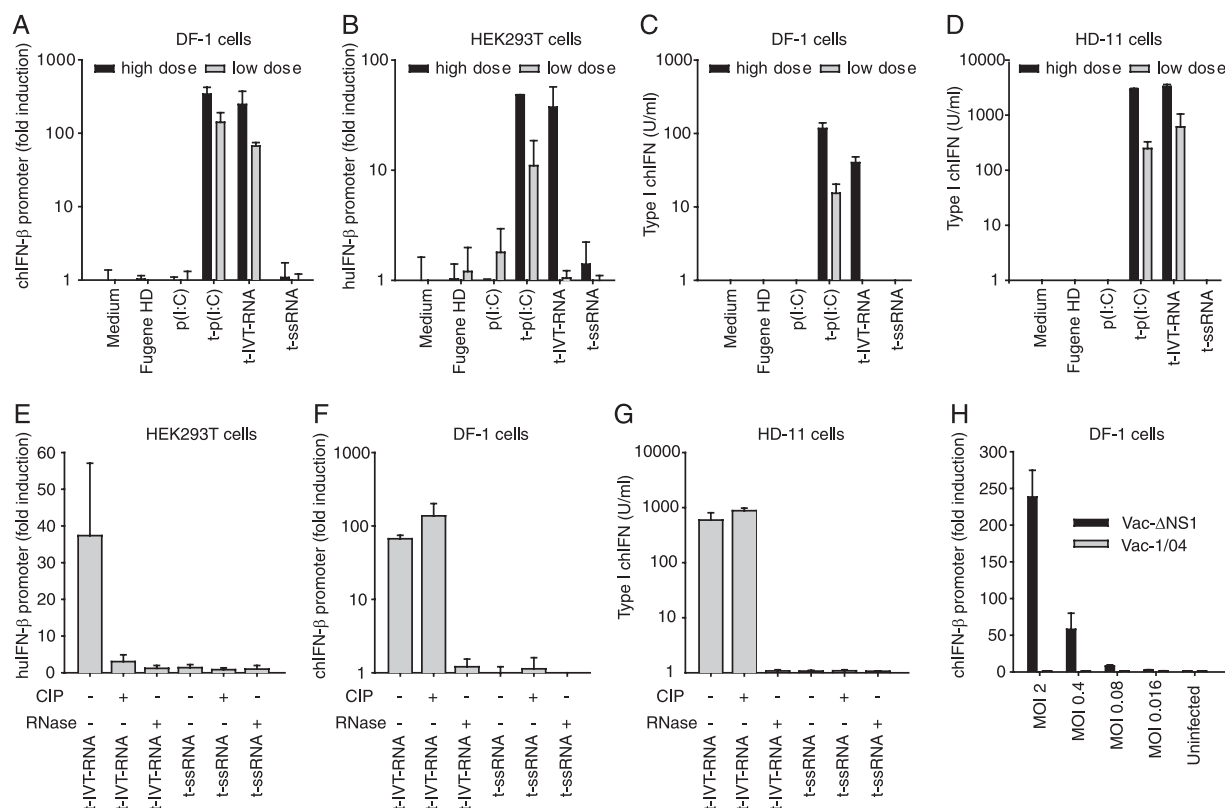
FIG 1 Type I interferon responses of chicken cells stimulated with ssRNA and dsRNA analogues. The effect of dsRNA and ssRNA (A to D), of triphosphorylated ssRNA (E to G), and of AIV (H) on IFN-β promoter induction (A, B, E, F, and H) and on type I chIFN bioactivity (C, D, and G) were analyzed in chicken DF-1 fibroblast cells (A, C, F, and H), in chicken macrophage-like HD-11 cells (D and G), and in human HEK293T cells (B and E). The induction of the IFN-β promoter-dependent firefly luciferase was normalized to that of Renilla luciferase and expressed as fold induction compared to that of unstimulated cells. The type I chIFN in the supernatant was quantified with the bioassay. For the analysis of type I IFN induction by dsRNA and ssRNA (A to D), the cells were stimulated with 2 μg/ml (high dose) and 0.5 μg/ml (low dose) of p(I:C) or t-p(I:C), with 1 μg/ml (high dose) and 0.25 μg/ml (low dose) of t-IVT-RNA, or with synthetic ssRNA of the same sequence (t-ssRNA). (E to G) The IVT-RNA and ssRNA concentrations were 0.25 μg/ml for DF-1 and HD-11 cells and 1 μg/ml for HEK293T cells. The cells were stimulated with t-IVT-RNA or with t-ssRNA that were previously dephosphorylated with calf intestinal phosphatase (CIP+) or digested with an RNase cocktail (RNase+) or the untreated RNAs (−), as indicated. (H) DF-1 cells were transfected with chIFN-β promoter reporters prior to infection with AIV. The data are representative of at least two independent experiments performed in triplicate wells, with the bars representing the mean values and the error bars showing the standard deviations.

1F and G). The response to dephosphorylated t-IVT-RNA was dependent on the presence of RNA, as the RNase treatment abolished the induction of type I IFN (Fig. 1E to G). These data suggest that DF-1 and HD-11 cells sense IVT-RNA by intracellular RIG-I-like receptors independently of the 5′-ppp moieties, as opposed to human HEK293T cells.

DF-1 cells respond to danger signals mediated by H5N1 AIV. The infection of DF-1 cells with LPAIV Vac-1/04 (Fig. 1H) and HPAIV Yamaguchi-7/04 (data not shown) did not activate the chIFN-β promoter regardless of the multiplicity of infection (MOI). However, a recombinant Vac-1/04 virus lacking the entire NS1 gene (Vac-ΔNS1) induced a strong upregulation of the chIFN-β promoter in an MOI-dependent manner (Fig. 1H). This shows that DF-1 cells can sense AIV in the absence of RIG-I. Importantly, wild-type Vac-1/04 counteracts the activation of type I chIFN by means of the NS1 protein, as expected from previous reports (27, 45).

Identification, cloning, and sequence analysis of the putative chicken CARDIF and chicken LGP2. To characterize the RLR signaling pathway involved in the induction of type I chIFN in chicken cells, we sought to characterize chicken genes coding for potential

CARD-like domains similar to those found in the mammalian RIG-I, MDA5, and CARDIF proteins. We identified a putative chicken ortholog (GenBank accession number NP_001012911.1) of the mammalian CARDIF based on a BLASTP search of the chicken genome reference protein database at NCBI using the murine CARDIF amino acid sequence. This protein was previously described in a phylogenic tree of known and predicted CARDIF proteins from various species but not further characterized (55). Therefore, we cloned and sequenced the open reading frame of the putative chCARDIF and deposited the nucleotide sequence in GenBank (accession number HQ845772). Forty percent identity was found for the N-terminal 95 amino acids that form the characteristic CARD domain present in mammalian CARDIF proteins (39). The Conserved Domain Database (CDD) at NCBI (http://www.ncbi.nlm.nih.gov/cdd) predicts a CARD domain (CARD_IPS1 [cd08811]) from amino acids 5 to 88 of the putative chCARDIF. Apart from the putative N-terminal CARD domain that is conserved from pufferfish to human, the amino acid sequence alignment of CARDIF revealed only limited identity between the full-length chicken protein and the human and mouse CARDIF sequences (26.3 and 21.7% identity, respectively). We
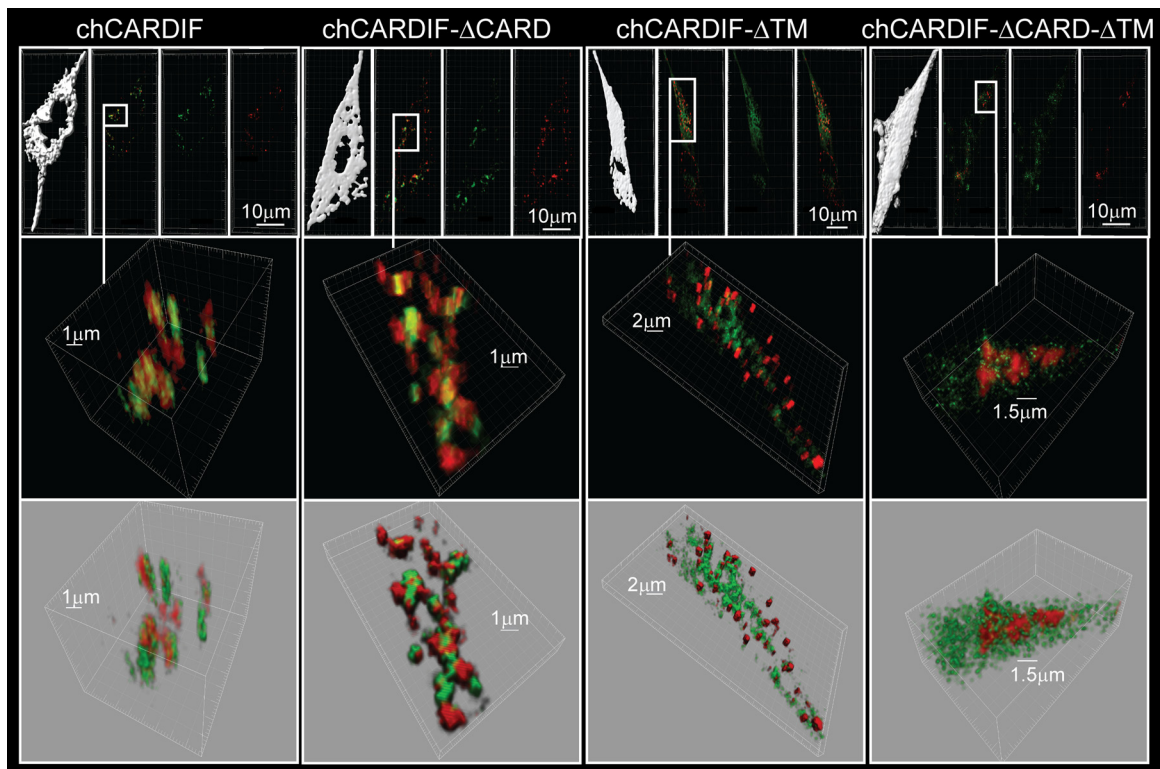
FIG 2 Putative chCARDIF localizes to the mitochondria. DF-1 cells were cotransfected with plasmid pHcRed1-Mito together with plasmids expressing N-terminally HT7-tagged chCARDIF (chCARDIF), HT7-tagged chCARDIF with deleted N-terminal CARD domain (chCARDIF-ΔCARD), HT7-tagged chCARDIF with deleted C-terminal TM (chCARDIF-ΔTM), or HT7-tagged chCARDIF with both CARD and TM deleted (chCARDIF-ΔCARD-ΔTM). The red fluorescence of the HcRed1 protein and the green fluorescence of the HaloTag R110 direct ligand covalently bound to HT7-tagged protein were analyzed by confocal microscopy with the Imaris 7.2 software program. The top row shows micrographs obtained by combining a series of sections taken for the selected cell to create a 3D image; this is shown as the whole cell (depicted using the Surface analysis module of Imaris 7.2), overlapping green and red fluorescence in this cell, green fluorescence alone, and red fluorescence alone (reading from left to right). The second micrograph for each construct shows a small box which depicts the region of the zoomed image shown in the middle and bottom rows. This middle row shows a maximum intensity projection (MIP) display of the image in 3D, while the bottom row shows a shadow projection display of the image in 3D. The MIP and shadow projection displays have been turned to give a clear appreciation of the positioning of the two colors: a few degrees for the chCARDIF and chCARDIF-ΔCARD images, 180° for the chCARDIF-ΔTM image, and 90° for the chCARDIF-ΔCARD-ΔTM image. The scale bars represent 5 to 10 μm in the top row and 1 to 2 μm in the middle and bottom rows, as indicated.

also identified a closely related putative CARDIF sequence from the zebra finch (Taeniopygia guttata; GenBank accession number XP_002188030.1) that shares 49% amino acid identity with the full-length putative chCARDIF. SMART analysis (http://smart.embl-heidelberg.de/) and the TMHMM server v. 2.0 (http://www.cbs.dtu.dk/services/TMHMM-2.0/) were used to predict TM domains in the putative chicken CARDIF protein sequence. The two software programs identified a C-terminal TM domain spanning from amino acids 617 to 636, which is consistent with the mammalian CARDIF proteins being mitochondrial transmembrane proteins. A proline-rich region was found in the central region of the putative chCARDIF, which is also in agreement with the mammalian CARDIF.

We also identified expressed sequence tags (ESTs) of a putative chicken LPG2 (chLGP2) based on similarities with mammalian LGP2 terminal sequences. The open reading frame of the putative chLGP2 was cloned and entirely sequenced. The nucleotide sequence was deposited in GenBank under the accession number HQ845773. The putative chLGP2 gene encodes a protein of 674 amino acids with 53 and 52% identity with human and mouse LGP2, respectively. Consistently with mammalian LGP2, CDD analysis revealed that chLGP2 also is devoid of any CARD domain

and consists of a DEAD-like helicase superfamily domain (DEXDc [cd00046]; from amino acids 18 to 170), a helicase superfamily C-terminal domain (HELICc [cd00079]; amino acids 344 to 470), and the RIG-I regulatory domain (RIG-I_C-RD [pfam11648]; amino acids 549 to 666).

The putative chCARDIF is associating with mitochondria. Confocal microscopy was used to analyze the subcellular localization of the putative chCARDIF. To this end, we expressed N-terminally HT7-tagged chCARDIF (HT7-chCARDIF), as well as HT7-tagged chCARDIF devoid of the N-terminal CARD-like domain (HT7-chCARDIF-ΔCARD), the C-terminal transmembrane domain (HT7-chCARDIF-ΔTM), or both (HT7-chCARDIF-ΔCARD-ΔTM). Wild-type and mutant putative chCARDIF proteins were expressed at similar levels, as determined by Western blot analysis using a specific polyclonal anti-HT7 antiserum (data not shown). The plasmid pHcRed1-Mito, encoding far-red fluorescent protein HcRed1 fused to a mitochondrial targeting sequence, was cotransfected with the sequences described above for visualization of the mitochondria. The green fluorescent HT7-tagged chCARDIF was clearly seen to be associating with the red fluorescent mitochondria (Fig. 2). This was visualized by the overlapping of the two fluorescences (top row). The green chCARDIF is seen to be asso-
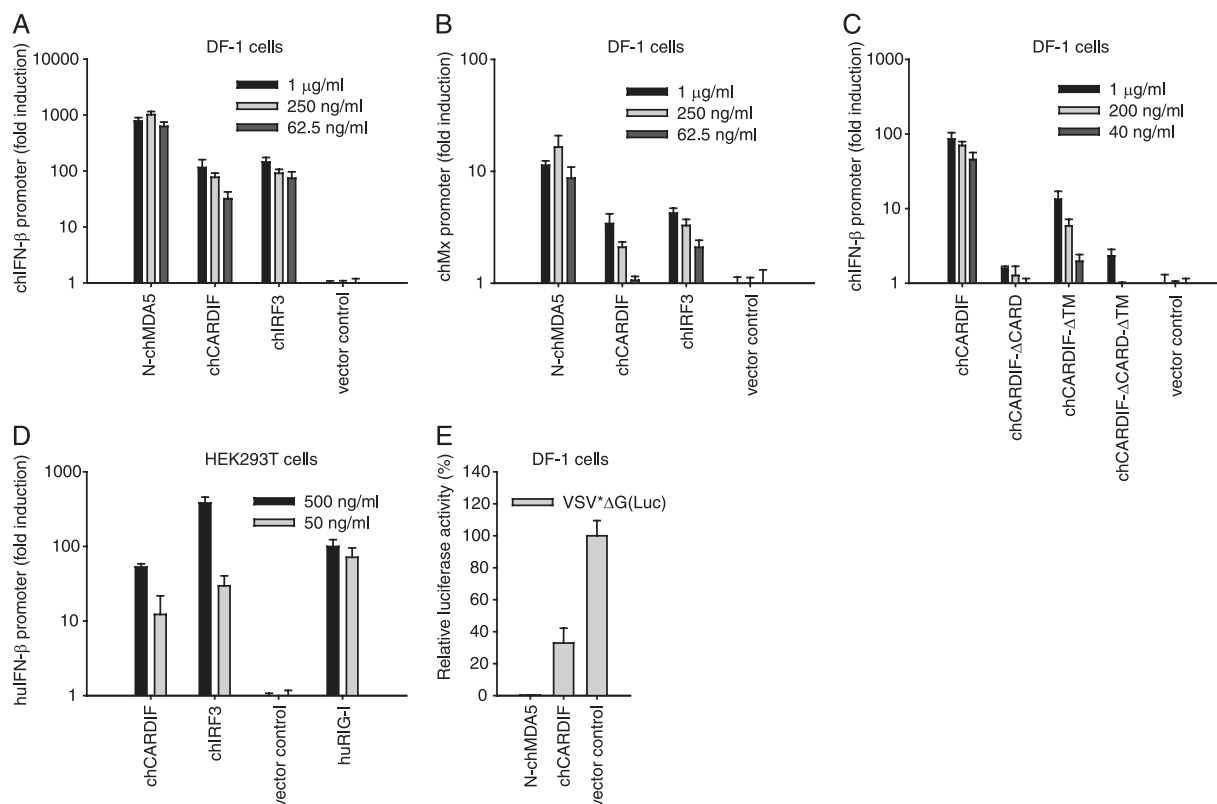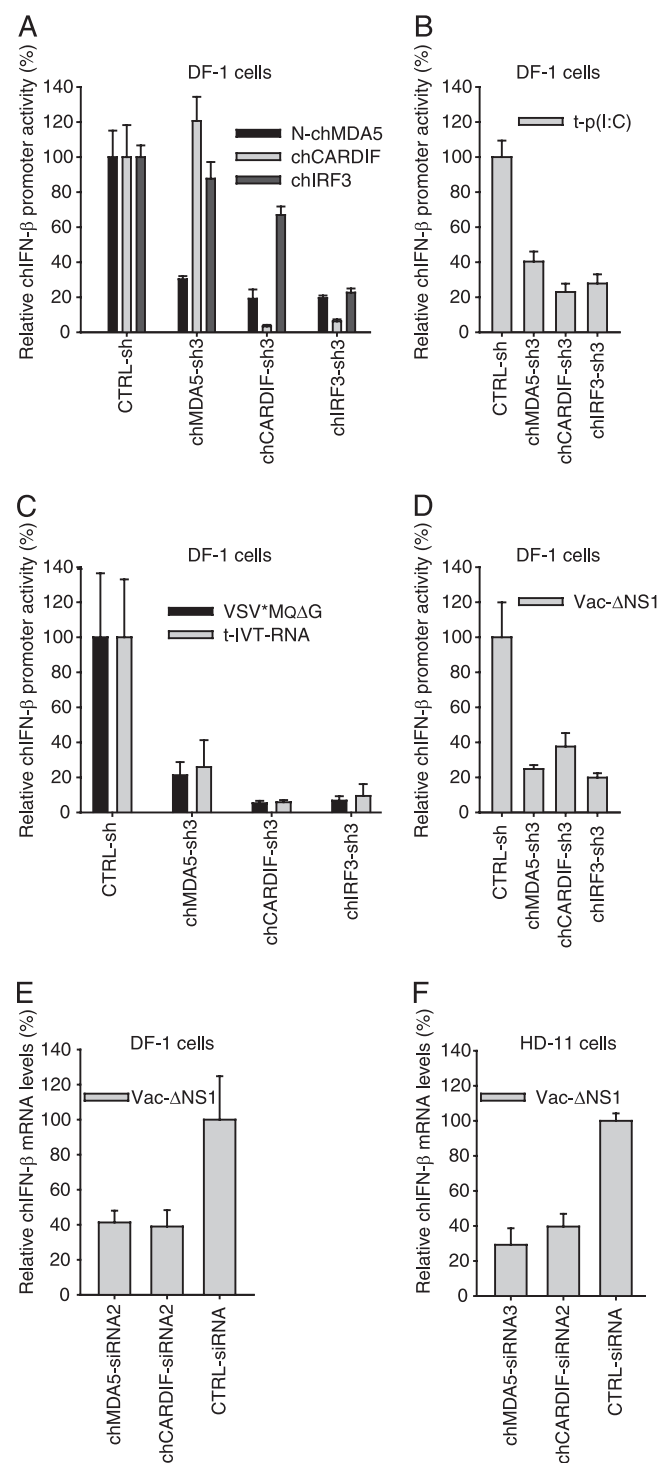
FIG 3 chCARDIF is an activator of type I IFN. The impact of the exogenous expression of the putative chCARDIF on the chIFN-β (A and C) and chMx (B) promoters in DF-1 cells, on the huIFN-β promoter in HEK293T cells (D), and on the establishment of an antiviral state in DF-1 cells (E) is shown. Promoter reporter assays were performed by the cotransfection of the indicated reporter plasmids together with decreasing amounts of plasmids expressing the N-terminal CARD domains of chMDA5 (N-chMDA5), putative chCARDIF, chIRF3, or empty plasmid as a vector control (A and B). (C) Using the same approach, chCARDIF was compared to mutants lacking the putative CARD domain (chCARDIF-ΔCARD), the predicted transmembrane domain (chCARDIF-ΔTM), or the two domains (chCARDIF-ΔCARD-ΔTM). (D) HEK293T cells were cotransfected with plasmids to conduct the human IFN-β reporter assay and with chCARDIF or chIRF3. The expression of human RIG-I (huRIG-I) served as a positive control. (A to D) The firefly and Renilla luciferase activities were determined after overnight incubation and expressed relative to vector control-transfected cultures. (E) DF-1 cells were transfected with chCARDIF or N-chMDA5 (both 1 μg/ml) and 18 h later were infected with a luciferase-expressing VSV replicon [VSV∗ΔG(Luc); MOI, 10] for 8 h. Data were obtained from quadruplicate transfections and are representative of at least two independent experiments.

ciated with the red mitochondria in the three-dimensional (3D) images (middle and bottom rows). The rotation of the image confirmed this interpretation (data not shown). The deletion of the CARD domain from chCARDIF gave images exemplified by those shown in the second panel of Fig. 2 (chCARDIF-ΔCARD). These demonstrated that in the absence of the CARD domain, the green chCARDIF still could associate with the red mitochondria. Zooming in on the boxed area marked on the second micrograph in the top row again showed a close association in the 3D images obtained. Indeed, one could not distinguish the degree of association between CARD-deleted chCARDIF and mitochondria from that observed with the intact chCARDIF, suggesting that chCARDIF does not require the intact CARD domain to associate with mitochondria. In contrast to the deletion of the CARD domain, the truncation of the C-terminal TM domain of the putative chCARDIF did disrupt mitochondrial association. This can be seen most clearly with the zoomed MIP and shadow projection 3D images (Fig. 2, chCARDIF-ΔTM, middle and bottom rows). The green chCARDIF is more dispersed, appearing to be cytosolic rather than organelle associated. Some of the green fluorescence appears close to the red mitochondrial label, but this is likely to be juxtapositioning by chance due to the dispersed cytosolic-like lo-

calization of chCARDIF-ΔTM. Certainly there is no intense organelle-like staining of the green CARDIF together with the red mitochondria, as was clearly observed with the intact chCARDIF or CARD-deleted chCARDIF (Fig. 2, chCARDIF and chCARDIF-ΔCARD). This was confirmed using the double deletion of CARD and TM (Fig. 2, chCARDIF-ΔCARD-ΔTM), which again showed a more cytosolic pattern of green fluorescence for chCARDIF. These results indicate a critical requirement of the TM domain in chCARDIF for appropriate mitochondrial association.

The N terminus of chMDA5 and of the putative chCARDIF are involved in type I IFN induction in DF-1 cells. The cytomegalovirus (CMV)-promoter-driven expression of the N-terminal 642 amino acids of the chMDA5 encompassing the CARD domains (N-chMDA5), of the putative chCARDIF, and of chIRF3 elicited a potent induction of the chIFN-β and chMx promoters in transfected DF-1 cells (Fig. 3A and B). Similarly, the transfection of the CEC-32 Mx reporter cells with plasmid constructs for the expression of N-chMDA5, the putative chCARDIF, and chIRF3 resulted in the induction of Mx-driven luciferase expression (data not shown). The expression of the putative chCARDIF lacking the CARD domain (chCARDIF-ΔCARD) failed to induce the chIFN-β promoter (Fig. 3C). Also, the truncation of the predicted
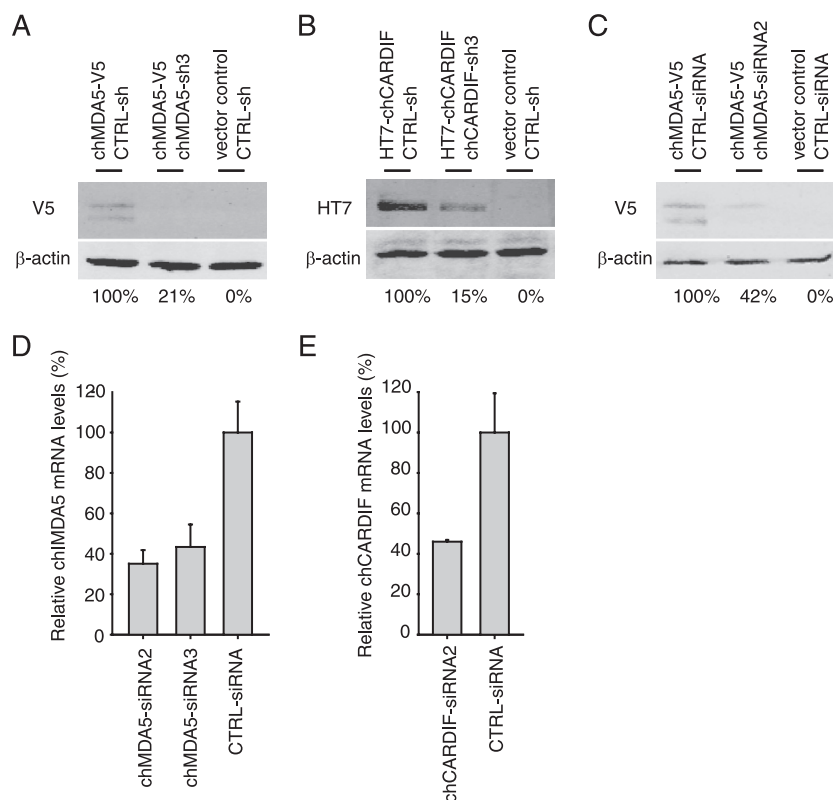
C-terminal TM domain (chCARDIF-ΔTM) resulted in approximately 10-fold reduced activity. As expected, the putative chCARDIF lacking the CARD and the TM domains did not activate the chIFN-β induction pathway (Fig. 3C). Interestingly, the putative chCARDIF and chIRF3 activated the human IFN-β promoter in HEK293T cells with levels comparable to those of human RIG-I (Fig. 3D). To elaborate on the functional relevance of the type I chIFN inductions measured above, we showed that the plasmid-driven expression of N-chMDA5 and of the putative chCARDIF was sufficient to inhibit the replication of a recombinant vesicular stomatitis virus replicon, VSV*ΔG(Luc), expressing firefly luciferase (Fig. 3E). Taken together, these data strongly suggest that the protein identified as putative chCARDIF is part of the type I chIFN induction cascade, in analogy to the mammalian CARDIF.

The putative chCARDIF mediates type I chIFN induction downstream of chMDA5 and upstream of chIRF3. The mammalian CARDIF functions downstream of RIG-I and MDA5 and upstream of IRF3 in the type I IFN induction cascade (46). To verify whether this also applies to the putative chCARDIF in chicken cells, the activation of the chIFN-β promoter in DF-1 cells was analyzed after the silencing of chMDA5, chCARDIF, and chIRF3 gene expression using the pRFPRNAiC-driven synthesis of specific shRNA (Fig. 4A). The silencing of chMDA5 significantly reduced the activation of the chIFN-β promoter mediated by the overexpression of N-chMDA5 but not by the overexpression of the putative chCARDIF or chIRF3. The shRNA targeting the putative chCARDIF substantially decreased chIFN-β promoter induction in cells stimulated with the expression of N-chMDA5 and the putative chCARDIF itself but had only a minor effect in cells stimulated with chIRF3. Finally, the shRNA targeting of chIRF3 abolished chIFN-β activation with all three stimuli. A control shRNA composed of a random, nontargeting sequence did not have any effect on the promoter activity induced by N-chMDA5, chCARDIF, and chIRF3 overexpression. Taken together, these data demonstrate that the putative chCARDIF represents the chicken analog of the mammalian CARDIF, functioning downstream of the RLR and upstream of chIRF3.

chMDA5, chCARDIF, and chIRF3 are required for virus-mediated type I IFN induction in DF-1 cells. Gene silencing also was applied to determine the requirement of chMDA5, chCARDIF, and chIRF3 in response to danger signals mediated by virus infections. To this end, dsRNA, triphosphorylated ssRNA, a

using pcDNA6-derived constructs (A); with t-p(I:C) (1.5 μg/ml) (B); with t-IVT-RNA (0.5 μg/ml) or with VSV*M$_Q$ΔG infection (MOI, 10) (C); and with Vac-ΔNS1 infection (MOI, 10) (D). After 18 h, a dual-luciferase assay was performed. Results were obtained from four (A and C) or six (B and D) experiments. The data were expressed relative to the luciferase activity in DF-1 cells transfected with nontargeting pRFPRNAiC-CTRL-sh set to 100%. Error bars indicate standard deviations. In cells transfected with pRFPRNAiC CTRL-sh plasmid, the fold induction above that of unstimulated cells with t-p(I:C), t-IVT RNA, VSV replicon, and Vac-ΔNS1 were 57 (±5.3 SD), 69.9 (±23.1), 9.5 (±3.4), and 76 (±15.1), respectively. (E and F) DF-1 and HD-11 cells were transfected with specific siRNA targeting chMDA5 or chCARDIF or with random control siRNA (CTRL-siRNA) as indicated. The cells then were infected with Vac-ΔNS1 or mock infected. Relative chIFN-β mRNA levels were assessed by quantitative real-time RT-PCR analysis 6 h after infection. Average mRNA levels derived from infected cells treated with CTRL-siRNA were set to 100%. Experiments were performed in quadruplicate. Error bars indicate standard deviations. The differences between the effects observed from targeting siRNA and CTRL-siRNA were statistically significant (t test).

FIG 4 chMDA5, chCARDIF, and chIRF3 are required to sense viral danger signals in chicken cells. (A to D) The influence of the shRNA-mediated silencing of chMDA5, chCARDIF, and chIRF3 on the induction of the chIFN-β promoter reporter was analyzed in DF-1 cells. (E and F) The effects of siRNA-based silencing of chMDA5 and chCARDIF on AIV-induced chIFN-β mRNA induction were examined in DF-1 and HD-11 cells. (A to D) The cells were cotransfected with pRFPRNAiC-derived plasmids (at 1 μg/ml) for shRNA transcription as indicated and with reporter plasmids for chIFN-β promoter activity. Note that the shRNA directed against chMDA5 is targeted to the 5′-terminal region of the mRNA. The cells were stimulated with the expression of N-chMDA5 (100 ng/ml), chCARDIF (200 ng/ml), or chIRF3 (200 ng/ml)

FIG 5 Validation of shRNA- or siRNA-mediated silencing of chMDA5 and chCARDIF gene expression. Specific shRNA-mediated (A and B) and siRNA-mediated (C to E) knockdowns of target gene expression were investigated in chicken DF-1 cells. (A and B) The cells were cotransfected with control vector or with plasmids expressing either C-terminal V5-tagged chMDA5 (chMDA5-V5) (A) or N-terminal HT7-tagged chCARDIF (HT7-chCARDIF) (B) together with the indicated pRFPRNAiC-derived plasmids for the transcription of specific or random control shRNAs (all plasmids were at 0.5 μg/ml). After 2 days, the expression levels of tagged chMDA5 and chCARDIF were quantified by Western blotting and immunodetection using anti-V5 antibody or anti-HT7 polyclonal serum. For normalization purposes, the β-actin content was determined with anti-β-actin MAb. The relative signal intensity measured in the presence of gene-specific shRNA is indicated as a percentage of the signal measured with CTRL-shRNA. (C) Cells were transfected with chMDA5-V5 or the vector control (at 0.5 μg/ml) for 6 h, followed by siRNA transfections as indicated. Two days later, the relative protein expression level of chMDA5-V5 was quantified by Western blot analysis as described for panels A and B. (D and E) Cells were transfected with specific siRNA targeting chMDA5 or chCARDIF or with random control siRNA (CTRL-siRNA) as indicated. Two days after transfection, the endogenous chMDA5 (D) or chCARDIF (E) mRNA levels were assessed by quantitative real-time RT-PCR and normalized to the 18S RNA content. The average normalized mRNA levels measured in cells treated with CTRL-siRNA were set to 100%. Transfections were performed in quadruplicate. Error bars indicate standard deviations. The differences between the effects observed with siRNA and CTRL-siRNA were statistically significant (t test).

VSV replicon, and an AIV lacking NS1 were used as triggers. As expected, chMDA5, chCARDIF, and chIRF3 all were required for chIFN-β promoter induction by t-p(I:C) (Fig. 4B) and t-IVT-RNA, mimicked the viral PAMP (Fig. 4C). Accordingly, the silencing of chMDA5, chCARDIF, and chIRF3 also prevented the chIFN-β promoter induction by VSV*M_QΔG (Fig. 4C) and by AIV Vac-ΔNS1 (Fig. 4D). To extend this study to chicken macrophages, we evaluated the effects of siRNA-based chMDA5 and chCARDIF silencing on AIV-induced chIFN-β mRNA induction in HD-11 cells. As expected from the previous experiments, the siRNA targeting of chMDA5 and chCARDIF significantly reduced chIFN-β mRNA expression induced by AIV Vac-ΔNS1 infection in DF-1 and HD-11 cells (Fig. 4E and F).

The effectiveness of shRNA- and siRNA-mediated silencing of gene expression was analyzed in DF-1 cells by Western blotting and quantitative RT-PCR (Fig. 5). With shRNA, tagged chMDA5 and chCARDIF proteins were efficiently downregulated (Fig. 5A and B). The siRNA-mediated silencing of chMDA5 reduced the protein and mRNA levels by approximately 60% (Fig. 5C and D). The mRNA level of chCARDIF was reduced to a similar extent by

siRNA treatment (Fig. 5E). Collectively, the gene-silencing experiments demonstrate the requirement of chMDA5, chCARDIF, and chIRF3 for sensing RNA virus infections in chicken cells.

chLGP2 is required for type I chIFN induction in DF-1 and HD-11 cells. The LGP2 helicase regulates RIG-I- and MDA5-mediated responses in mammals (40, 42). The downregulation of the putative chLGP2 in DF-1 and HD-11 cells reduced type I chIFN secretion (Fig. 6A and B), indicating that chLGP2 functions are required for chRLR signaling. On average, the supernatants of Vac-ΔNS1-infected DF-1 and HD-11 cells contained 7.7 U/ml (±1.6 standard deviations [SD]) and 8.2 U/ml (±0.9 SD) of type I chIFN 18 and 6 h after infection, respectively. Moreover, the gene-silencing experiments altogether demonstrate the requirement of chMDA5, putative chLGP2, chCARDIF, and chIRF3 for AIV-mediated type I IFN induction in chicken cells. The siRNA-mediated silencing of tagged chLGP2 protein is demonstrated in Fig. 6C. In mammalian cells, LGP2 negatively regulates RLR-mediated signaling when it is overexpressed (40). Therefore, we tested whether this also applies to the putative chLGP2. As expected, the expression of the putative chLGP2 interfered with the
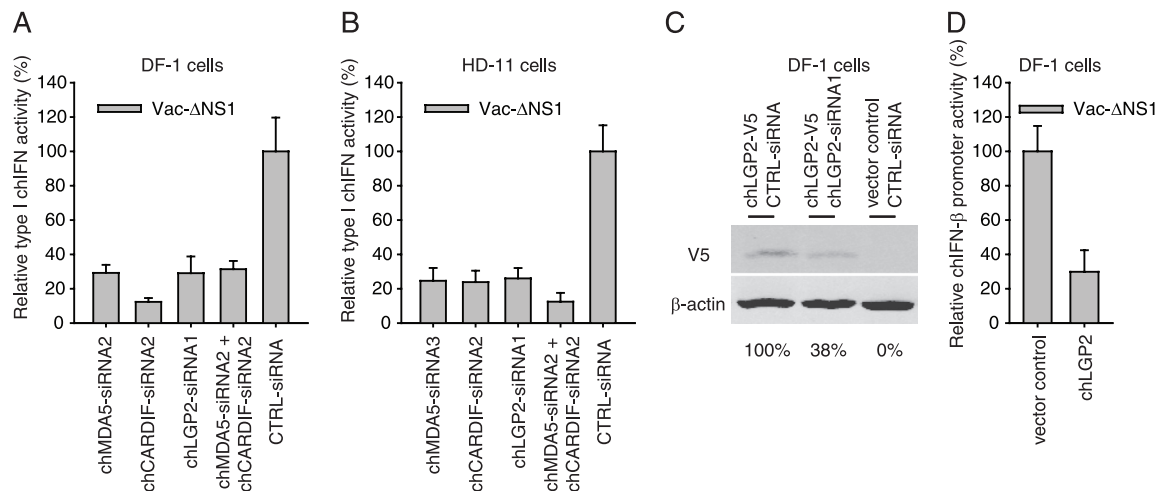
FIG 6 chLGP2 is a functional element of the chIFN-β activation pathway in DF-1 and HD-11 cells. (A and B) The effects of siRNA-based silencing of chMDA5, chCARDIF, and chLGP2 on AIV-induced chicken type I IFN secretion were analyzed in DF-1 and HD-11 cells.(C) The siRNA-mediated silencing of chLGP2 gene expression was analyzed. (D) The effect of chLGP2 overexpression on the Vac-ΔNS1-mediated induction of the chIFN-β promoter was determined in DF-1 cells. For silencing, DF-1 (A) and HD-11 cells (B) were transfected with specific siRNA targeting chMDA5, chCARDIF, or chLGP2 or with random control siRNA (CTRL-siRNA) as indicated. At 18 (A) or 6 h (B) after Vac-ΔNS1 infection, type I chIFN was quantified using the CEC32-based bioassay. The bioactivity was expressed relative to the mean values measured from infected and CTRL-siRNA-transfected cells set to 100%. Experiments were performed in quadruplicate. Error bars indicate standard deviations. The differences between the effects observed from targeting siRNA and CTRL-siRNA were statistically significant (t test). To demonstrate the downregulation of chLGP2 by siRNA, DF-1 cells were transfected with pcDNA6-chLGP2-V5 (at 0.5 μg/ml) or empty vector (vector control) (at 0.5 μg/ml) for 6 h, followed by siRNA transfections as indicated. Two days later, protein expression levels were quantified by Western blotting and immunodetection using the anti-V5 antibody. The β-actin content was determined with the anti-β-actin MAb. To assess the effect of chLGP2 overexpression on IFN-β promoter activation, DF-1 cells were cotransfected with constant amounts of reporter plasmids and with pcDNA6-chLGP2 (at 0.5 μg/ml) or empty vector (vector control). (D) After 24 h, the cells were stimulated with Vac-ΔNS1 (MOI, 5) or left untreated for another 24 h before performing the dual-luciferase assay. Experiments were performed in quadruplicate. Data are expressed as percentages of the levels obtained with the corresponding nonstimulated cells. The normalized luciferase levels obtained with the parent vector DNA were set to 100%.

Vac-ΔNS1-driven activation of the chicken RLR pathway (Fig. 6D), indicating that the gene identified as putative chLGP2 indeed functions similarly to the mammalian LGP2.

H5N1 AIV counteracts the chicken RLR signaling pathway by means of the NS1 protein. Recently, an alanine-to-valine mutation at position 149 (A149V) of the NS1 gene of the HPAIV A/goose/Guangdong/1/96 (H5N1) was reported to abolish the counteraction of AIV-mediated type I IFN induction in chicken fibroblasts (27). The mutant virus was attenuated in chicken. We introduced this mutation into the NS1 gene from the HPAIV Yamaguchi-7/04 and the LPAIV Vac-1/04 at positions 144 and 149, respectively, corresponding to position 149 described above. The expression of the parent NS1 proteins of the two viruses but not of the respective mutant proteins significantly impaired the t-p(I:C)-mediated activation of the chIFN-β promoter in DF-1 cells independently of the V5 tag (Fig. 7A). Vac-ΔNS1-mediated chIFN-β promoter activation also was impaired by the NS1 protein of the Yamaguchi-7/04 virus but was only partially blocked by the A144V mutant (Fig. 7B). The expression of the native NS1 as opposed to the NS1-A144V mutant also prevented the N-chMDA5-mediated induction of the chIFN-β promoter in DF-1 cells (Fig. 7C). The IRF3-mediated chIFN-β promoter induction also was partially reduced by NS1 but not by NS1-A144V. With the tagged proteins, comparable levels of protein expression were demonstrated (Fig. 7D). In HEK293T cells, however, both the parent and the mutant NS1 proteins suppressed the huRIG-I- and huMDA5-mediated activation of the human IFN-β promoter (Fig. 7E). In summary, these data show that NS1 of H5N1 AIV inhibits RLR-mediated IFN-β induction in chicken and human cells.

DISCUSSION

In the present study, we characterized the chicken RLR pathway by defining the role of chMDA5, chLGP2, chCARDIF, and chIRF3 in the recognition of viral PAMP, particularly that of AIV. We identified the chCARDIF and chLGP2 coding sequences and demonstrated the functions of their products in chMDA5-mediated signaling and type I IFN induction. The expression of chLGP2 interferes with chMDA5-specific signaling. Finally, we showed that the MDA5-mediated signaling was inhibited by NS1 of an H5N1 AIV but not of a mutant NS1 (A144V).

Our results indicate that human and chicken RLR pathways respond in a fashion similar to that of the stimulation with dsRNA but differ in comparisons of 5'-pppRNA to dephosphorylated RNA. Unlike the human cells, the two chicken cells respond to both the 5'-pppRNA and the dephosphorylated RNA, indicating that chicken generally lack the capacity to specifically sense only 5'-ppp RNA structures, as shown for RIG-I in mammalian cells. As IVT-RNA is known to contain dsRNA structures (43, 44), the type I chIFN response observed in t-IVT-RNA-stimulated chicken cells might be due to dsRNA structures. Our data employing MDA5 gene knockdown performed in chicken DF-1 and HD-11 cells indicate that chMDA5 represents the principle intracellular PRR mediating AIV and intracellular dsRNA recognition. Considering that in mammals RIG-I acts as the main cytosolic PRR involved in sensing influenza virus infections (24) and that chickens lack RIG-I (2, 62), this indicates that the chMDA5 can functionally compensate for the absence of RIG-I in the chicken genome. Furthermore, the potent activation of the chIFN-β promoter by the infection of DF-1 cells with a recombinant H5N1
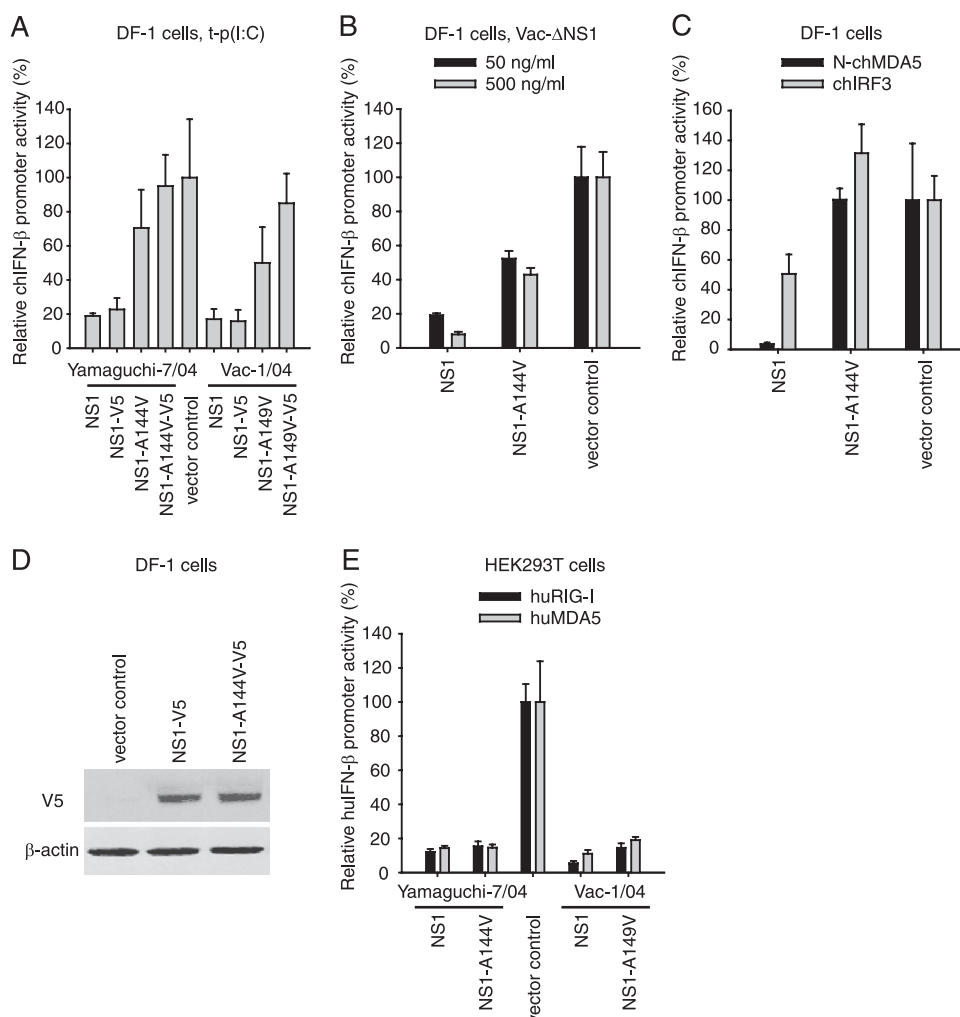
FIG 7 H5N1 AIV NS1 interferes with chIFN type I induction. The effect of the AIV NS1 protein on the chIFN-β promoter (A to C) was analyzed in DF-1 cells stimulated with t-p(I:C) (A), with Vac-ΔNS1 (B), or with the expression of N-chMDA5 or chIRF3 (C). (E) In comparison, the effect of the AIV NS1 protein on the huIFN-β promoter was characterized in HEK293T cells stimulated with huRIG-I or huMDA5 expression. (A) The cells were cotransfected with constant amounts of chIFN-β reporter plasmids and with pcDNA6 expressing V5-tagged or untagged parent or mutant NS1 from Yamaguchi-7/04 or Vac-1/04 or with the empty vector (all expression plasmids were at 0.5 μg/ml). (B) The cells were cotransfected with the chIFN-β reporter plasmids and with pcDNA6 expressing NS1 or NS1-A144V of Yamaguchi-7/04, or with the empty vector, at 50 ng/ml and 0.5 μg/ml as indicated. After 24 h, the cells were stimulated with 2 μg/ml t-p(I:C) (A) or with Vac-ΔNS1 virus at an MOI of 10 (B). (C) DF-1 cells were cotransfected with the chIFN-β reporter plasmids and with pcDNA6 constructs expressing N-chMDA5 (50 ng/ml) or chIRF3 (0.5 μg/ml) as indicated, pcDNA6 plasmid expressing NS1 or NS1-A144V, or with the empty vector (all NS1 expression plasmids and the vector control were at 0.5 μg/ml). Dual-luciferase assays were performed after 18 h. Stimulations were performed in quadruplicate. The levels obtained with parent vector DNA were set to 100%. (D) The expression of the V5-tagged wild-type and mutant Yamaguchi-7/04 NS1 proteins was analyzed by Western blotting using the anti-V5 MAb. The β-actin content was determined with the anti-β-actin MAb. (E) HEK293T cells were cotransfected with huIFN-β reporter plasmids together with the empty pcDNA6 vector or pcDNA6 expressing huRIG-I or huMDA5 (as stimuli) and with pcDNA6 expressing intact or mutant NS1 of Yamaguchi-7/04 and Vac-1/04. The empty pcDNA6 vector served as a control (vector control). Dual-luciferase assays with quadruplicate transfections were performed after 24 h. The relative huIFN-β promoter activity was expressed as the percentage of activity obtained with empty pcDNA6.

AIV lacking the NS1 gene does not support the hypothesis that the lack of RIG-I represents a reason for the increased susceptibility of chickens to AIV compared to the susceptibility of ducks that have the RIG-I gene. Nevertheless, resolving this question would require *in vivo* investigations, for instance, employing transgenic chicken expressing duck RIG-I.

In the present study, we also identified the chCARDIF that is associated with mitochondria like its mammalian counterpart. The overexpression of chCARDIF and chIRF3 triggered IFN type I responses in chicken as well as in mammalian cells, pointing to the functional conservation of these molecules during evolution.

This was surprising, given the low degree of amino acid identity of the two chicken genes with their mammalian counterparts. As expected, gene-silencing experiments revealed that chCARDIF acts downstream of chMDA5 and upstream of chIRF3. As with mammalian CARDIF, the association with mitochondria and the activation of the IFN-β promoter were found to be dependent on the predicted C-terminal TM domain, whereas the putative N-terminal CARD domain was found to be indispensable for downstream signaling. Surprisingly, the TM-deficient chCARDIF retained approximately 10% of the activity of the full-length chCARDIF, which may be explained by the residual binding of the

truncated protein to the mitochondria, as observed by microscopy. Finally, gene-silencing experiments in chicken cells demonstrate that chCARDIF is required for AIV-induced type I IFN responses. Similarly, we also show that the chIRF3 transcription factor is required for chRLR-mediated type I IFN responses, as expected from mammalian RLR pathways (21). Consistently with MDA5 in mammalian systems (1, 8), the overexpression of a polypeptide containing the twin CARD domains of chMDA5 (N-chMDA5) activated the chIFN-β promoter. LGP2 knockdown experiments in chicken cells demonstrate that chLGP2 is essential to mediate RLR-specific antiviral responses, as described for human LGP2 (42, 54), but again, similarly to human (40), chLGP2 overexpression negatively interfered with AIV-induced innate immune signaling in chicken cells.

In mammals, one of the multiple reported functions of the influenza A NS1 protein is to antagonize the RIG-I-specific induction of type I IFNs (12, 15, 32, 35). In analogy with this, we show that in the chicken system NS1 interferes with the chMDA5-mediated pathway. The NS1 deletion mutant but not the wild-type AIV activated the type I IFN pathway, and plasmid-expressed NS1 suppressed chMDA5-mediated chIFN-β promoter activation. The finding that the expression of NS1 also moderately decreased chIRF3-induced chIFN-β promoter responses may reflect other functions exerted by the multifunctional NS1 protein, such as the general suppression of host gene expression.

In conclusion, we demonstrate that the intracellular chMDA5 pathway represents a key anti-AIV innate immune recognition pathway in chicken cells. Chicken and mammalian RLR pathways share the common components MDA5, LGP2, CARDIF, and IRF3, but unlike the case in mammals, chMDA5 possesses the capacity to sense AIV, apparently in a 5′-ppp-independent manner. Whether the failure of chickens to specifically sense viral 5′-ppp PAMPs helps to explain the increased susceptibility of chickens to AIV compared to that of ducks remains to be investigated. It also could be speculated that such species-dependent differences in innate immune recognition has an effect on virus evolution in different animals.

ACKNOWLEDGMENTS

REFERENCES

1. **Andrejeva J, et al.** 2004. The V proteins of paramyxoviruses bind the IFN-inducible RNA helicase, mda-5, and inhibit its activation of the IFN-beta promoter. Proc. Natl. Acad. Sci. U. S. A. **101**:17264–17269.
2. **Barber MR, Aldridge Jr, Jr, Webster RG, Magor KE.** 2010. Association of RIG-I with innate immunity of ducks to influenza. Proc. Natl. Acad. Sci. U. S. A. **107**:5913–5918.
3. **Berger Rentsch M, Zimmer G.** 2011. A vesicular stomatitis virus replicon-based bioassay for the rapid and sensitive determination of multi-species type I interferon. PLoS One **6**:e25858.
4. **Beug H, von Kirchbach A, Doderlein G, Conscience JF, Graf T.** 1979. Chicken hematopoietic cells transformed by seven strains of defective avian leukemia viruses display three distinct phenotypes of differentiation. Cell **18**:375–390.
5. **Binder M, Kochs G, Bartenschlager R, Lohmann V.** 2007. Hepatitis C virus escape from the interferon regulatory factor 3 pathway by a passive and active evasion strategy. Hepatology **46**:1365–1374.
6. **Caldwell RB, et al.** 2005. Full-length cDNAs from chicken bursal lymphocytes to facilitate gene function analysis. Genome Biol. **6**:R6.
7. **Cardona CJ, Xing Z, Sandrock CE, Davis CE.** 2009. Avian influenza in birds and mammals. Comp. Immunol. Microbiol. Infect. Dis. **32**:255–273.
8. **Childs K, et al.** 2007. mda-5, but not RIG-I, is a common target for paramyxovirus V proteins. Virology **359**:190–200.
9. **Cui S, et al.** 2008. The C-terminal regulatory domain is the RNA 5′-triphosphate sensor of RIG-I. Mol. Cell **29**:169–179.
10. **Das RM, et al.** 2006. A robust system for RNA interference in the chicken using a modified microRNA operon. Dev. Biol. **294**:554–563.
11. **Fredericksen BL, Keller BC, Fornek J, Katze MG, Gale M, Jr.** 2008. Establishment and maintenance of the innate antiviral response to West Nile virus involves both RIG-I and MDA5 signaling through IPS-1. J. Virol. **82**:609–616.
12. **Gack MU, et al.** 2009. Influenza A virus NS1 targets the ubiquitin ligase TRIM25 to evade recognition by the host viral RNA sensor RIG-I. Cell Host Microbe **5**:439–449.
13. **Gitlin L, et al.** 2010. Melanoma differentiation-associated gene 5 (MDA5) is involved in the innate immune response to Paramyxoviridae infection in vivo. PLoS Pathog. **6**:e1000734.
14. **Grant CE, Vasa MZ, Deeley RG.** 1995. cIRF-3, a new member of the interferon regulatory factor (IRF) family that is rapidly and transiently induced by dsRNA. Nucleic Acids Res. **23**:2137–2146.
15. **Guo Z, et al.** 2007. NS1 protein of influenza A virus inhibits the function of intracytoplasmic pathogen sensor, RIG-I. Am. J. Respir. Cell Mol. Biol. **36**:263–269.
16. **Hoffmann E, Krauss S, Perez D, Webby R, Webster RG.** 2002. Eight-plasmid system for rapid generation of influenza virus vaccines. Vaccine **20**:3165–3170.
17. **Hoffmann M, et al.** 2010. Fusion-active glycoprotein G mediates the cytotoxicity of vesicular stomatitis virus M mutants lacking host shut-off activity. J. Gen. Virol. **91**:2782–2793.
18. **Hornung V, et al.** 2006. 5′-Triphosphate RNA is the ligand for RIG-I. Science **314**:994–997.
19. **Isoda N, et al.** 2006. Pathogenicity of a highly pathogenic avian influenza virus, A/chicken/Yamaguchi/7/04 (H5N1) in different species of birds and mammals. Arch. Virol. **151**:1267–1279.
20. **Jorns C, et al.** 2006. Rapid and simple detection of IFN-neutralizing antibodies in chronic hepatitis C non-responsive to IFN-alpha. J. Med. Virol. **78**:74–82.
21. **Juang YT, et al.** 1998. Primary activation of interferon A and interferon B gene transcription by interferon regulatory factor 3. Proc. Natl. Acad. Sci. U. S. A. **95**:9837–9842.
22. **Karpala AJ, Stewart C, McKay J, Lowenthal JW, Bean AG.** 2011. Characterization of chicken Mda5 activity: regulation of IFN-beta in the absence of RIG-I functionality. J. Immunol. **186**:5397–5405.
23. **Kato H, et al.** 2008. Length-dependent recognition of double-stranded ribonucleic acids by retinoic acid-inducible gene-I and melanoma differentiation-associated gene 5. J. Exp. Med. **205**:1601–1610.
24. **Kato H, et al.** 2006. Differential roles of MDA5 and RIG-I helicases in the recognition of RNA viruses. Nature **441**:101–105.
25. **Kawai T, et al.** 2005. IPS-1, an adaptor triggering RIG-I- and Mda5-mediated type I interferon induction. Nat. Immunol. **6**:981–988.
26. **Li X, et al.** 2009. Structural basis of double-stranded RNA recognition by the RIG-I like receptor MDA5. Arch. Biochem. Biophys. **488**:23–33.

27. **Li Z, et al.** 2006. The NS1 gene contributes to the virulence of H5N1 avian influenza viruses. J. Virol. **80**:11115–11123.

28. **Long JX, Peng DX, Liu YL, Wu YT, Liu XF.** 2008. Virulence of H5N1 avian influenza virus enhanced by a 15-nucleotide deletion in the viral nonstructural gene. Virus Genes **36**:471–478.

29. **Loo YM, et al.** 2008. Distinct RIG-I and MDA5 signaling by RNA viruses in innate immunity. J. Virol. **82**:335–345.

30. **Malik Peiris JS.** 2009. Avian influenza viruses in humans. Rev. Sci. Tech. **28**:161–173.

31. **Meylan E, et al.** 2005. Cardif is an adaptor protein in the RIG-I antiviral pathway and is targeted by hepatitis C virus. Nature **437**:1167–1172.

32. **Mibayashi M, et al.** 2007. Inhibition of retinoic acid-inducible gene I-mediated induction of beta interferon by the NS1 protein of influenza A virus. J. Virol. **81**:514–524.

33. **Moulin HR, et al.** 2011. High interferon type I responses in the lung, plasma and spleen during highly pathogenic H5N1 infection of chicken. Vet. Res. **42**:6.

34. **Neumann G, Chen H, Gao GF, Shu Y, Kawaoka Y.** 2010. H5N1 influenza viruses: outbreaks and biological properties. Cell Res. **20**:51–61.

35. **Opitz B, et al.** 2007. IFNbeta induction by influenza A virus is mediated by RIG-I which is regulated by the viral NS1 protein. Cell. Microbiol. **9**:930–938.

36. **Pantin-Jackwood MJ, Swayne DE.** 2009. Pathogenesis and pathobiology of avian influenza virus infection in birds. Rev. Sci. Tech. **28**:113–136.

37. **Peters MA, Browning GF, Washington EA, Crabb BS, Kaiser P.** 2003. Embryonic age influences the capacity for cytokine induction in chicken thymocytes. Immunology **110**:358–367.

38. **Pichlmair A, et al.** 2006. RIG-I-mediated antiviral responses to single-stranded RNA bearing 5′-phosphates. Science **314**:997–1001.

39. **Potter JA, Randall RE, Taylor GL.** 2008. Crystal structure of human IPS-1/MAVS/VISA/Cardif caspase activation recruitment domain. BMC Struct. Biol. **8**:11.

40. **Rothenfusser S, et al.** 2005. The RNA helicase Lgp2 inhibits TLR-independent sensing of viral replication by retinoic acid-inducible gene-I. J. Immunol. **175**:5260–5268.

41. **Ruggli N, et al.** 2005. N(pro) of classical swine fever virus is an antagonist of double-stranded RNA-mediated apoptosis and IFN-alpha/beta induction. Virology **340**:265–276.

42. **Satoh T, et al.** 2010. LGP2 is a positive regulator of RIG-I- and MDA5-mediated antiviral responses. Proc. Natl. Acad. Sci. U. S. A. **107**:1512–1517.

43. **Schlee M, et al.** 2009. Recognition of 5′ triphosphate by RIG-I helicase requires short blunt double-stranded RNA as contained in panhandle of negative-strand virus. Immunity **31**:25–34.

44. **Schmidt A, et al.** 2009. 5′-Triphosphate RNA requires base-paired structures to activate antiviral signaling via RIG-I. Proc. Natl. Acad. Sci. U. S. A. **106**:12067–12072.

45. **Schwarz H, Harlin O, Ohnemus A, Kaspers B, Staeheli P.** 2004. Synthesis of IFN-beta by virus-infected chicken embryo cells demonstrated with specific antisera and a new bioassay. J. Interferon Cytokine Res. **24**:179–184.

46. **Seth RB, Sun L, Ea CK, Chen ZJ.** 2005. Identification and characterization of MAVS, a mitochondrial antiviral signaling protein that activates NF-kappaB and IRF 3. Cell **122**:669–682.

47. **Sick C, et al.** 1998. Promoter structures and differential responses to viral and nonviral inducers of chicken type I interferon genes. J. Biol. Chem. **273**:9749–9754.

48. **Soda K, et al.** 2008. Development of vaccine strains of H5 and H7 influenza viruses. Jpn. J. Vet. Res. **55**:93–98.

49. **Takahasi K, et al.** 2009. Solution structures of cytosolic RNA sensor MDA5 and LGP2 C-terminal domains: identification of the RNA recognition loop in RIG-I-like receptors. J. Biol. Chem. **284**:17465–17474.

50. **Takahasi K, et al.** 2008. Nonself RNA-sensing mechanism of RIG-I helicase and activation of antiviral immune responses. Mol. Cell **29**:428–440.

51. **Takeuchi O, Akira S.** 2009. Innate immunity to virus infection. Immunol. Rev. **227**:75–86.

52. **Takeuchi O, Akira S.** 2008. MDA5/RIG-I and virus recognition. Curr. Opin. Immunol. **20**:17–22.

53. **Takeuchi O, Akira S.** 2007. Recognition of viruses by innate immunity. Immunol. Rev. **220**:214–224.

54. **Venkataraman T, et al.** 2007. Loss of DExD/H box RNA helicase LGP2 manifests disparate antiviral responses. J. Immunol. **178**:6444–6455.

55. **Wang D, et al.** 2008. Molecular cloning and functional characterization of porcine IFN-beta promoter stimulator 1 (IPS-1). Vet. Immunol. Immunopathol. **125**:344–353.

56. **Xing Z, et al.** 2011. Host immune and apoptotic responses to avian influenza virus H9N2 in human tracheobronchial epithelial cells. Am. J. Respir. Cell Mol. Biol. **44**:24–33.

57. **Xu LG, et al.** 2005. VISA is an adapter protein required for virus-triggered IFN-beta signaling. Mol. Cell **19**:727–740.

58. **Yoneyama M, Fujita T.** 2010. Recognition of viral nucleic acids in innate immunity. Rev. Med. Virol. **20**:4–22.

59. **Yoneyama M, Fujita T.** 2009. RNA recognition and signal transduction by RIG-I-like receptors. Immunol. Rev. **227**:54–65.

60. **Yoneyama M, et al.** 2004. The RNA helicase RIG-I has an essential function in double-stranded RNA-induced innate antiviral responses. Nat. Immunol. **5**:730–737.

61. **Yoneyama M, et al.** 1996. Autocrine amplification of type I interferon gene expression mediated by interferon stimulated gene factor 3 (ISGF3). J. Biochem. **120**:160–169.

62. **Zou J, Chang M, Nie P, Secombes CJ.** 2009. Origin and evolution of the RIG-I like RNA helicase gene family. BMC Evol. Biol. **9**:85.